

# Synthesis and Optical Properties of Solid and Hollow ZnO Microspheres Prepared by Hydrothermal Method

Lite ZHAO<sup>1</sup>, Fu DAI<sup>1\*</sup>, Donghua FAN<sup>1</sup>, Yizhan CHEN<sup>1</sup>, Chunlai ZHENG<sup>2</sup>, Zirong YANG<sup>1</sup>, Zeyan ZHUANG<sup>1</sup>, Kexin PI<sup>1</sup>, Jingquan MO<sup>1</sup>, Jingui DENG<sup>1</sup>

<sup>1</sup> Department of Applied physics and materials, Wuyi University, Jiangmen 529020, China

<sup>2</sup> School of Physics and Telecommunication Engineering, Shaanxi University of Technology 723000, China

**crossref** <http://dx.doi.org/10.5755/j01.ms.24.4.19141>

Received 27 September 2017; accepted 14 January 2018

We successfully synthesized solid and hollow ZnO microspheres by a template-free hydrothermal method on the substrate of porous alumina membranes. The morphology of prepared sample was characterized by scanning electron microscopy and transmission electron microscopy. The growth mechanism of the synthesized ZnO microspheres is discussed in detail. At step 1, solid ZnO microspheres were prepared by the thermal decomposition of the Zn(OH)<sub>2</sub> microspheres synthesized under the mixture of Zn(NO<sub>3</sub>)<sub>2</sub>·6H<sub>2</sub>O, C<sub>6</sub>H<sub>12</sub>N<sub>4</sub>, and C<sub>6</sub>H<sub>5</sub>Na<sub>3</sub>O<sub>7</sub>·2H<sub>2</sub>O solution. The quantity of C<sub>6</sub>H<sub>5</sub>Na<sub>3</sub>O<sub>7</sub>·2H<sub>2</sub>O dopant will greatly affect the morphology of the prepared sample by controlling ZnO nucleation and growth rate. At step 2, hollow ZnO microspheres were prepared by removing the Zn(OH)<sub>2</sub> cores in an alkaline solution. The proper pH value also plays a key role in preparing hollow ZnO microspheres with high quality. Compared with hollow nanostructure, the solid ZnO microsphere shows the relatively strong Raman peaks at 437 cm<sup>-1</sup>, which suggests that the prepared solid spheres should have the better crystal quality. Photoluminescence spectra show that the solid ZnO microspheres have the relatively strong ultraviolet (UV) peak at ~ 380 nm attributed to the recombination of free exciton, and the weak green peak owing to the low surface-to-volume ratio.

**Keywords:** ZnO microsphere, growth mechanism, optical properties.

## 1. INTRODUCTION

Recently, the synthesis of micro- and nanospheres has attracted much attention owing to their some properties, including unique architecture, high surface to volume ratio, and so on. It had been found that they can be applied in energy-storage media, artificial cells, drug-delivery carriers, etc. [1–4]. In recent years, ZnO has attracted great attention because it is an important semiconductor material and have the outstanding optical and electronic properties [5–7]. Structurally, zinc and oxygen atoms alternatively stack along the c-axis direction, which induces two positively-charged (0001)-Zn and negatively-charged (000 $\bar{1}$ )-O polar surfaces in ZnO crystal [8, 9]. Therefore, it is difficult to obtain ZnO micro- and nanospheres because ZnO has three fast growth directions of [0001], [10 $\bar{1}$ 0], and [2 $\bar{1}$  $\bar{1}$ 0].

At present, it has been reported that there are main two methods to prepare spherical ZnO structures, such as a template-assisted hydrothermal approach and thermal evaporation method [10–12]. Some materials have been used as templates, such as silica, polymer, or carbon spheres, vesicles, emulsions, micelles, or even gas bubbles. Generally, the template-assisted hydrothermal method includes two processes, i.e. coating and removal of template. Therefore, the preparation of ZnO microspheres requires a sophisticated multi-step synthetic procedure and complex formula. To overcome the aforementioned problems, some scientists used the thermal evaporation method to prepare ZnO spherical structures. Umar *et al.*

prepared spherical ZnO microstructures by heating the mixture of Zn and ZnCl<sub>2</sub> powder at high temperature [13]. Lu *et al.* researched the growth process of the ZnO microberets synthesized by thermal evaporation methods [14]. Fan *et al.* also detailedly researched the influence of oxygen flow on the morphology and optical properties of the synthesized ZnO hollow microspheres by thermal evaporation process [15]. Compared with a template-assisted hydrothermal approach, the thermal evaporation technique generally is simply without complex process. However, the preparation of sample during the thermal evaporation process needs the high temperatures and vacuum conditions in general. It is obvious that the high heating temperature is not helpful for the application of ZnO microsphere. Therefore, there is still challenge that using a simple and economical route to synthesize spherical ZnO structures.

In this paper, solid and hollow ZnO microspheres were successfully prepared by a template-free hydrothermal method on the substrate of porous alumina membranes (PAMs). The observations of scanning electron microscopy (SEM) and transmission electron microscopy (TEM) confirm that the prepared samples consist of solid or hollow ZnO microsphere. By comparison with the morphologies of samples synthesized at different reaction times and solutions, the growth mechanism of solid and hollow ZnO microsphere was discussed in detail. The optical properties of the synthesized samples also were investigated.

\* Corresponding author. Tel.: +750-3296307.  
E-mail address: [ioe\\_daif@126.com](mailto:ioe_daif@126.com) (F. Dai)

## 2. EXPERIMENTAL DETAILS

Step 1: we prepared respectively 8 mM Zn(NO<sub>3</sub>)<sub>2</sub>·6H<sub>2</sub>O, 8 mM C<sub>6</sub>H<sub>12</sub>N<sub>4</sub>, and 2.2 mM C<sub>6</sub>H<sub>5</sub>Na<sub>3</sub>O<sub>7</sub>·2H<sub>2</sub>O aqueous solution in different beakers before the experiment, then all of the configured solutions were transferred to a glass bottle. Immediately after, substrates were put into the solution. Before the experiment, we prepared PAMs through a typical two-step anodizing electrochemical procedure. During the experiment, the fabricated PAMs were used as substrate, and the glass bottle was sealed and heated in a laboratory oven. The heating temperature and time are 90 °C and 60 min, respectively. To testify the key role of C<sub>6</sub>H<sub>5</sub>Na<sub>3</sub>O<sub>7</sub>·2H<sub>2</sub>O, we prepared the samples without it at the same condition. After the experiment is over, all of the samples were removed from the solution, washed with deionized water repeatedly, and dried under the air. The prepared samples are used as the substrate at step 2. To synthesize the ZnO microsphere, the prepared samples were heated in the furnace at 200 °C for 60 min.

Step 2: in order to synthesize the hollow ZnO microspheres, we also prepared the following aqueous solution in different beakers, including 15 mM Zn(NO<sub>3</sub>)<sub>2</sub>·6H<sub>2</sub>O, 15 mM C<sub>6</sub>H<sub>12</sub>N<sub>4</sub>, and 4.5 mM C<sub>6</sub>H<sub>5</sub>Na<sub>3</sub>O<sub>7</sub>·2H<sub>2</sub>O, respectively. Subsequently, these three aqueous solutions were mixed in a glass bottle. In addition, by adding ammonia we also adjusted the pH value of the mixture solution to around 8. After solid ZnO microspheres prepared above were put into the mixture, the glass bottle was sealed and heated at 90 °C for 15, 30 and 45 min. In order to research the influence of pH values on the structure and morphology, we also prepared samples at pH = 10 and 12 at the same condition, respectively. After the experiment was over, all of the samples were removed from the solution, washed with deionized water repeatedly, and dried under the air.

In the experiment, both field-emission SEM (NoVaTM Nano SEM 430) and high resolution TEM (JEOL JEM-2100F) were used to characterize the morphology and structure of the prepared samples. We also measured the micro-Raman spectra by a Jobin Yvon LabRAM HR 800UV micro-Raman system under an Ar<sup>+</sup> (514.5 nm) ion laser. In addition, the photoluminescence (PL) spectra were measured using 325 nm UV line of a He-Cd laser as excitation source.

## 3. RESULTS AND DISCUSSION

In the experiment, the PAMs were used as the substrates. Fig. 1 a displays SEM images of the fabricated PAMs, where the surface of sample is uniform and consists of the hexagonal nanopore arrays with pore diameter of about 100 nm. Fig. 1 b gives the FE-SEM image of the prepared ZnO microspheres. Those samples were firstly prepared under the mixture solution, i.e. 8 mM Zn(NO<sub>3</sub>)<sub>2</sub>·6H<sub>2</sub>O, 8 mM C<sub>6</sub>H<sub>12</sub>N<sub>4</sub>, and 2.2 mM C<sub>6</sub>H<sub>5</sub>Na<sub>3</sub>O<sub>7</sub>·2H<sub>2</sub>O aqueous solution, and then heated under the furnace at 200 °C for 60 min. A number of solid ZnO microspheres were synthesized on the PAMs with diameters ranging from 1–2 μm. Fig. 1 c shows the corresponding TEM images, which suggests that the as-fabricated

microspheres are solid. The insert in Fig. 1(c) also displays the high-magnification TEM image, which further demonstrate the successful realization of solid microspheres. During the TEM measurements, we also performed energy-dispersive X-ray (EDX) spectroscopy analysis for the prepared samples, as shown in Fig. 1 d. Apart from the signal of Cu, it is obvious that the solid microspheres consist of Zn and O elements. Considering that in the experiment there is no introduction of Cu compound, the signal of Cu may come from the copper grid in the measurement of sample. Therefore, the SEM observation and EDX results testify the successful synthesis of solid ZnO microspheres.

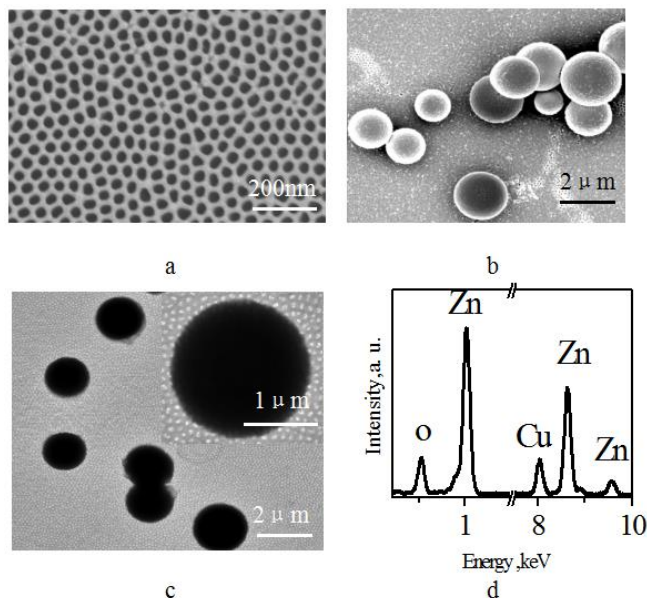


**Fig. 1.** a – FE-SEM image of the PAMs used as substrates; b – the FE-SEM image of the prepared sample under 8 mM Zn(NO<sub>3</sub>)<sub>2</sub>·6H<sub>2</sub>O, 8 mM C<sub>6</sub>H<sub>12</sub>N<sub>4</sub>, and 2.2 mM C<sub>6</sub>H<sub>5</sub>Na<sub>3</sub>O<sub>7</sub>·2H<sub>2</sub>O aqueous solution; c – the corresponding TEM images, the inset is high-magnification TEM image of single nanostructure; d – EDX spectrum of the corresponding sample

By using the microsphere prepared at step 1 as the substrate, the core/shell ZnO microstructures could be obtained at step 2, as shown in the Fig. 2 a. The pH value of solution, the heating time and temperature are 8, 15 min and 90 °C, respectively. It is obvious that ZnO microspheres show core/shell structures with the diameter of around 2 μm. In the experiment, we also synthesized the other samples by changing the heating time. Fig. 2 b shows SEM morphology of the samples synthesized at 30 min. Though there is not obvious change of surface morphology, the size of core in ZnO microspheres is obviously decreases. When the reaction time increases to 60 min, all of the cores in the microspheres were removed, and hollow ZnO microspheres can be prepared, as shown in Fig. 2 c. In the insert of Fig. 2 c one can clearly observe that the prepared microsphere has a hollow nature. Fig. 2 d displays TEM observation of the prepared samples at 60 min, where they consist of a light inner center and relative dark edge. This observation can further confirm that the obtained microspheres are hollow.

To research of the influence of C<sub>6</sub>H<sub>5</sub>Na<sub>3</sub>O<sub>7</sub> on the growth of nanostructure at step 1, we prepared the sample

in the absence of  $C_6H_5Na_3O_7$ . In the experiment, the other conditions were kept constant.

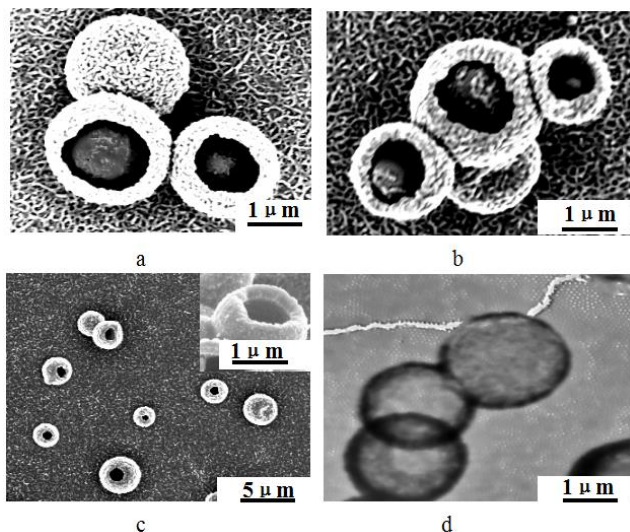


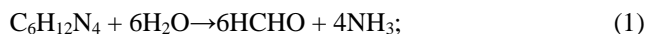
**Fig. 2.** a, b–SEM images of core/shell ZnO microspheres prepared under 90 °C at 15 and 30 min, respectively; c–SEM image of hollow ZnO microsphere prepared under 90 °C at 60 min. The insert is that of a single nanostructure. d–TEM image of the corresponding microsphere of c

In this case, not microsphere nanostructure but ZnO nanorods with the hexagonal-structure were formed, as shown in Fig. 3 a. With increasing a small quantity of  $C_6H_5Na_3O_7$ , ZnO nanorods with the hexagonal-structure will become shorter and fatter, as shown in Fig. 3 b. The insert shows the enlarged picture of a single microstructure. It shows that the prepared nanostructures have the hexagonal structure, thus suggesting the growth of the formed ZnO crystal along  $\langle 001 \rangle$  orientation. It is well known that there is a different growth rate in ZnO crystal along various lattice plane. It was reported that the 1-D ZnO nanostructures grow along  $[0001]$  direction in general because there is the relatively high growth rate in different ZnO crystal faces [16]. ZnO microsphere could be prepared by using a large enough amount of  $C_6H_5Na_3O_7$  in the experiment, as shown in Fig. 1 b. These observations indicate that the introduction of  $C_6H_5Na_3O_7$  could limit the growth rate of the  $\langle 001 \rangle$  direction in the formation of ZnO nanostructure and prompt the formation of spherical ZnO structure.

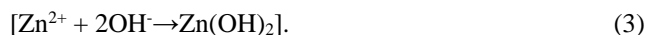
To research the influence of pH value on the growth of microsphere at step 2, we prepared the sample at various pH values with the other conditions kept the same. Fig. 3 c shows SEM image of hollow microspheres prepared at pH = 10. Compared with SEM image of the samples prepared at pH = 8 (Fig. 2 c), the morphology of ZnO microspheres is destroyed, and the cores and part of shells are dissolved. When the pH value increases to 12, there are no ZnO microspheres due to the dissolution of shells, as shown in Fig. 3 d. Those observations indicate that the high pH value not only leads to the disappearance of cores but also causes the dissolution of the shells. Therefore, the appropriate pH value should play a key role in the formation of ZnO microspheres with high quality.

According to the experimental results observed above, we can presume the growth process of solid and hollow ZnO

microspheres. At step 1, the used  $C_6H_{12}N_4$  plays a role to slowly release  $OH^-$  ions through thermal decomposition [17]:



In this process, the released  $OH^-$  ions will react with  $Zn^{2+}$  ions to prompt the formation of  $Zn(OH)_2$  nanoclusters in solution:



Therefore, solid  $Zn(OH)_2$  microspheres were prepared at present. When the prepared samples were heated at 200 °C for 60 min, ZnO microsphere can be fabricated by the heating decomposition of  $Zn(OH)_2$ :



The reaction process mentioned above does not involve  $C_6H_5Na_3O_7$ . Considering that the introduction of  $C_6H_5Na_3O_7$  leads to the change of morphology from nanorods to microspheres,  $C_6H_5Na_3O_7$  should play a key role to modulate the nucleation and growth rate in the growth of crystals. It also has reported that the citrate ions during the reaction could decrease the crystal growth rate along the  $\langle 001 \rangle$  orientation [18].

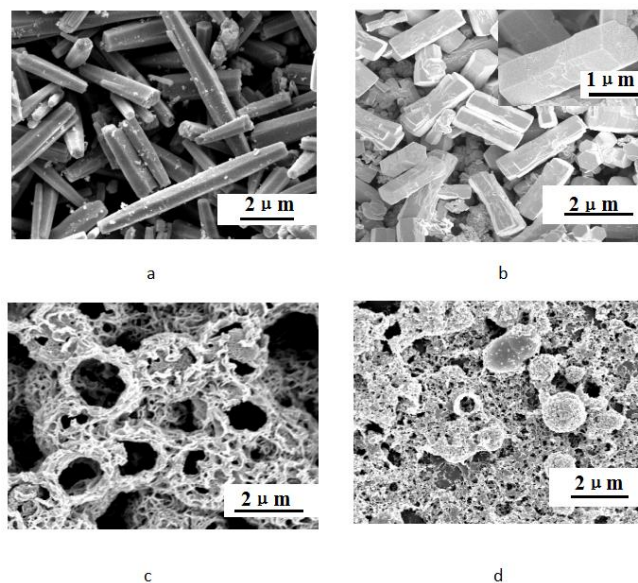


**Fig. 3.** a–SEM image of the prepared ZnO nanorods without  $C_6H_5Na_3O_7$  at step 1 b–SEM image of the prepared ZnO at a small quantity of  $C_6H_5Na_3O_7$ . The insert shows the enlarged picture of a single ZnO nanorod. c, d–the SEM images of ZnO hollow microspheres prepared at pH = 10 and 12 at step 2, respectively

Next, the growth process of hollow ZnO microsphere shall be discussed. When the solid microspheres prepared at step 1 were moved to a mixed solution at step 2, the yielded  $Zn(OH)_2$  will hydrolyze to yield ZnO layer on the surface of  $Zn(OH)_2$  microsphere due to the dissolution of  $Zn(OH)_2$  ( $Zn(OH)_2 \rightarrow ZnO + H_2O$ ), which leads to the core/shell structure. When the ammonia was added into solution,  $Zn(OH)_2$  cores in the microspheres can be dissolved ( $Zn(OH)_2 + 4NH_3 \rightarrow (Zn(NH_3)_4)_2 + 2OH^-$ ), which leads to the formation of hollow ZnO microsphere [18, 19]. With a

great deal of ammonia adding to the solution, we can observe that the morphology of microsphere become worse and worse, and even ZnO microsphere disappears. This is because the introduction of ammonia also dissolves ZnO shells. When a small amount of ammonia was added in the solution, the yielded ZnO can effectively equalize the loss on the shells, which prompts the preparation of hollow microsphere with perfect morphology. The incorporation of much ammonia could cause that the rate of dissolution is bigger than that of production of ZnO, which leads to the disappearance of a number of hollow ZnO microspheres.

Now, we have studied the optical properties of solid and hollow ZnO microspheres by room-temperature Raman and photoluminescence (PL) measurements. Fig. 4 a gives Raman spectra of the as-prepared solid and hollow ZnO microspheres, where it shows the peaks at  $\sim 380$ ,  $437$  and  $580\text{ cm}^{-1}$ , respectively. Both samples show the strong peaks at  $437\text{ cm}^{-1}$ , which suggests that they have better crystal quality. According to the group theory, part of optic modes in the ZnO nanomaterials are Raman active, i.e.  $A_1$ ,  $E_1$ , and  $2E_2$  [20, 21]. Therefore, the observed modes at  $\sim 380$ ,  $437$  and  $580\text{ cm}^{-1}$  in Fig. 4 a should be assigned to the  $A_1$  (TO),  $E_2$  (high), and  $E_1$  (LO), respectively [20]. Compared with the hollow ZnO microspheres, the prepared solid spheres show the relatively strong Raman peak at  $437\text{ cm}^{-1}$ , which suggests that it should have better crystal quality. Generally,  $E_1$  (LO) mode at  $\sim 580\text{ cm}^{-1}$  is related to the oxygen vacancies [22]. The hollow ZnO microspheres display the relatively strong the Raman shift at  $\sim 580\text{ cm}^{-1}$ , suggesting that there is more deficiency due to the relatively more superficial area.

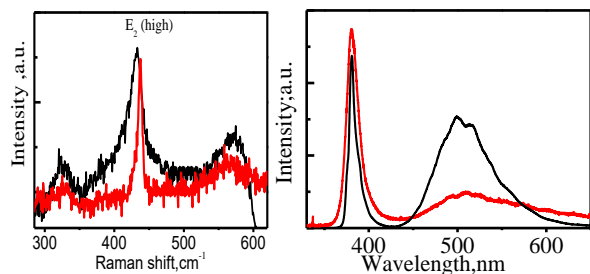


**Fig. 4.** a, b – Raman and PL spectra of the prepared samples, where the red and black curves are corresponding to solid and hollow ZnO microspheres, respectively

The optical properties of ZnO microspheres have also been investigated by PL spectroscopy. Fig. 4 b shows the PL emission of solid and hollow ZnO microspheres. The red and black curves are corresponding to the emission spectra of solid and hollow ZnO microspheres, respectively. It is obvious that there are two peaks, i.e. UV emission at  $\sim 380\text{ nm}$  and a green one at  $\sim 510\text{ nm}$ . It was reported that the UV peak around  $380\text{ nm}$  is normally called near band edge NBE peak [23]. Compared with the hollow microspheres, there is the relatively strong UV peak at solid ones, which suggests the relatively good crystal quality in solid ZnO nanostructures. As for the green emission at  $\sim 510\text{ nm}$ , it was reported that it should be attributed to the singly ionized oxygen vacancies or the intrinsic defect [24, 25]. Considering that the observation of Raman spectra, we deduce that the singly ionized oxygen vacancies cause the green peak. In addition, the high surface-to-volume ratio

can prompt the formation of more oxygen vacancies [26], which leads to the strong green peak at the hollow microspheres.

## 4. CONCLUSIONS

Solid and hollow ZnO microspheres successfully were synthesized by a template-free hydrothermal method on the substrate of PAMs. SEM and TEM observations were used to characterize the morphology of prepared samples. By comparison with the images of samples prepared at different reaction times and solutions, the growth process of hollow and solid ZnO microstructures was discussed in detail. At step 1,  $\text{Zn}(\text{OH})_2$  microspheres firstly were prepared, and then we synthesized ZnO solid ones by the thermal decomposition. Though the  $\text{C}_6\text{H}_5\text{Na}_3\text{O}_7 \cdot 2\text{H}_2\text{O}$  does not react with any compound in solution, it plays a key role in preparing ZnO microspheres by controlling its nucleation and growth rate. If there is no  $\text{C}_6\text{H}_5\text{Na}_3\text{O}_7$  in the reaction, the prepared samples only show ZnO nanorods with hexagonal structure. At step 2, ZnO hollow microspheres were prepared by removing the  $\text{Zn}(\text{OH})_2$  cores by adding an alkaline in the solution, where pH value is 8. The appropriate pH value also plays a key role in the growth of ZnO microspheres with high quality. The high pH value not only leads to the disappearance of cores but also causes the dissolution of shells. Compared with hollow microspheres, the solid ZnO nanostructure shows the relatively strong Raman peaks at  $437\text{ cm}^{-1}$ , which suggests that the prepared solid spheres should have the better crystal quality. PL emission of solid and hollow ZnO microspheres shows the strong UV peak at  $\sim 380\text{ nm}$  attributed to the recombination of free exciton, which suggests that there is the relatively good crystal quality. The strong green peak at the hollow microspheres should be correlated to more oxygen vacancies.

## Acknowledgements

This work was supported by Science Foundation for Young Teachers of Wuyi University (2015zk13), the Science and Technology Project of Jiangmen City (Jiang Ke [2016]189), the Characteristic Innovation Project of Department of Education of Guangdong Province (2014KTSCX129), and Young Creative Talents Project of Education Department in Guangdong Province (2015KQNCX170).

## REFERENCES

1. Liu, Y., Chu, Y., Zhuo, Y., Dong, L., Li, L., Li, M. Controlled Synthesis of Various Hollow Cu Nano/MicroStructures via a Novel Reduction Route *Advanced Functional Materials* 17 (6) 2010: pp.933–938. <https://doi.org/10.1002/adfm.200600333>
2. Blanco, I., Abate, L., Bottino, F.A. Synthesis and Thermal Properties of New Dumbbell-Shaped Isobutyl-Substituted POSSs Linked by Aliphatic Bridges *Journal of Thermal Analysis & Calorimetry* 116 (1) 2014: pp. 5–13. <http://dx.doi.org/10.1007/s10973-013-3487-3>
3. Sulieman, K.M., Huang, X., Tang, M. Controllable Synthesis and Characterization of Hollow-Opened ZnO/Zn and Solid Zn/ZnO Single Crystal Microspheres *Nanotechnology* 17 (19) 2006: pp. 4950–4955.

- <http://dx.doi.org/10.1088/0957-4484/17/19/029>
4. **Papathanassiou, A.N., Sakellis, I., Vitoratos, E., Sakkopoulos, S.** Interfacial and Space Charge Dielectric Effects in Polypyrrole/Zinc Oxide Composites *Synthetic Metals* 228 2017: pp.41–44.  
<https://doi.org/10.1016/j.synthmet.2017.03.019>
  5. **Ognibene, G., Cristaldi, D.A., Fiorenza, R., Blanco, I., Cicala, G., Scire, S., Fragalà, M.E.** Photoactivity of Hierarchically Nanostructured ZnO-PES Fibre Mats for Water Treatments *RSC Advances* 6 (49) 2016: pp. 42778–42785.  
<http://dx.doi.org/10.1039/c6ra06854e>
  6. **Salem, A.M.S., El-Sheikh, S.M., Harraz, F.A., Ebrahim, S., Soliman, M., Hafez, H.S., Ibrahim, I.A., Abdel-Mottaleb, M.S.A.** Inverted Polymer Solar Cell Based on MEH-PPV/PC61BM Coupled with ZnO Nanoparticles as Electron Transport Layer *Applied Surface Science* 425 2017: pp. 156–163.  
<https://doi.org/10.1016/j.apsusc.2017.06.322>
  7. **Multian, V.V., Uklein, A.V., Zaderko, A.N., Kozhanov, V.O., Boldyrieva, O.Y., Linnik, R.P., Lisnyak, V.V., Gayvoronsky, V.Y.** Synthesis, Characterization, Luminescent and Nonlinear Optical Responses of Nanosized ZnO *Nanoscale Research Letters* 12 (1) 2017: pp. 164–172.  
<https://doi.org/10.1186/s11671-017-1934-y>
  8. **Wang, Z.L., Kong, X.Y., Ding, Y., Gao, P.X., Hughes, W.L., Yang, R., Zhang, Y.** Semiconducting and Piezoelectric Oxide Nanostructures Induced by Polar Surfaces *Advanced Functional Materials* 14 (10) 2004: pp. 943–956.  
<http://dx.doi.org/10.1002/adfm.200400180>
  9. **Pan, Z.W., Dai, Z.R., Wang, Z.L.** Nanobelts of Semiconducting Oxides *Science* 291 2001: pp. 1947–1949.
  10. **Yu, T., Li, J., Xiong, H., Dai, J.** Controlled Synthesis of ZnO Hollow Microspheres via Precursor-Template Method and Its Gas Sensing Property *Applied Surface Science* 258 (22) 2012: pp. 8431–8438.  
<http://dx.doi.org/10.1016/j.apsusc.2011.12.090>
  11. **Li, Q., Wang, C., Ju, M., Chen, W., Wang, E.** Polyoxometalate-Assisted Electrochemical Deposition of Hollow ZnO Nanospheres and Their Photocatalytic Properties *Microporous & Mesoporous Materials* 138 (1) 2011: pp. 132–139.  
<http://dx.doi.org/10.1016/j.micromeso.2010.09.014>
  12. **Shen, G., Bando, Y., Lee, C.J.** Synthesis and Evolution of Novel Hollow ZnO Urchins by a Simple Thermal Evaporation Process *Journal of Physical Chemistry B* 109 (21) 2005: pp. 10578–10583.  
<https://pubs.acs.org/doi/abs/10.1021/jp051078a>
  13. **Umar, A., Kim, S.H., Im, Y.H., Hahn, Y.B.** Structural and Optical Properties of ZnO Micro-Spheres and Cages by Oxidation of Metallic Zn Powder *Superlattices & Microstructures* 39 (1–4) 2006: pp. 238–246.  
<https://doi.org/10.1016/j.spmi.2005.08.046>
  14. **Lu, H., Liao, L., Li, J., Wang, D., He, H., Fu, Q., Xu, L., Tian, Y.** High Surface-to-Volume Ratio ZnO Microberets: Low Temperature Synthesis, Characterization, and Photoluminescence *Journal of Physical Chemistry B* 110 (46) 2006: pp. 23211–23214.  
<http://dx.doi.org/10.1021/jp064079r>
  15. **Fan, D.H.** Synthesis of ZnO Hollow Spherical Structures with Different Surface-to-Volume Ratios *Applied Physics A* 96 (3) 2009: pp. 655–660.  
<https://doi.org/10.1007/s00339-009-5252-9>
  16. **Hu, J.Q., Bando, Y.** Growth and Optical Properties of Single-Crystal Tubular ZnO Whiskers *Applied Physics Letters* 82 (9) 2003: pp.1401–1403.  
<https://doi.org/10.1063/1.1558899>
  17. **Zhu, Y.F., Fan, D.H., Shen, W.Z.** Template-Free Synthesis of Zinc Oxide Hollow Microspheres in Aqueous Solution at Low Temperature *Journal of Physical Chemistry C* 111 (50) 2007: pp. 18629–18635.  
<https://pubs.acs.org/doi/10.1021/jp077573j>
  18. **Tian, Z.R., Voigt, J.A., Liu, J., Mckenzie, B., Mcdermott, M.J., Rodriguez, M.A., Konishi, H., Xu, H.** Complex and Oriented ZnO Nanostructures *Nature Materials* 2 (12) 2003: pp. 821–827.  
<https://doi.org/10.1038/nmat1014>
  19. **Ennaoui, A., Weber, M., Saad, M., Harneit, W., Lux Steiner, M.C., Karg, F.** Chemical Bath Deposited Zn(Se,OH)<sub>x</sub> on Cu(In,Ga)(S,Se)<sub>2</sub> for High Efficiency Thin Film Solar Cells: Growth Kinetics, Electronic Properties, Device Performance and Loss Analysis *Thin Solid Films* 361 2000: pp. 450–453.  
[https://doi.org/10.1016/S0040-6090\(99\)00815-9](https://doi.org/10.1016/S0040-6090(99)00815-9)
  20. **Wang, R.P., Xu, G., Jin, P.** Size Dependence of Electron-Phonon Coupling in ZnO Nanowires *Physical Review B* 69 (11) 2004: pp. 113303–113307.  
<https://doi.org/10.1103/PhysRevB.69.113303>
  21. **Calleja, J.M., Cardona, M.** Resonant Raman Scattering in ZnO *Physical Review B Condensed Matter* 16 (8) 1981: pp. 563–568.  
<http://dx.doi.org/10.1103/PhysRevB.16.3753>
  22. **Pan, H., Luo, J., Sun, H., Feng, Y., Poh, C., Lin, J.** Hydrogen Storage of ZnO and Mg Doped ZnO Nanowires *Nanotechnology* 17 (12) 2006: pp. 2963–2967.  
<http://dx.doi.org/10.1088/0957-4484/17/12/023>
  23. **Rackauskas, S., Mustonen, K., Järvinen, T., Mattila, M., Klimova, O., Jiang, H., Tolochko, O., Lipsanen, H., Kauppinen, E.I., Nasibulin, A.G.** Synthesis of ZnO Tetrapods for Flexible and Transparent UV Sensors *Nanotechnology* 23 (9) 2012: pp. 095502-1-7.  
<http://dx.doi.org/10.1088/0957-4484/23/9/095502>
  24. **Fan, D.H., Ning, Z.Y., Jiang, M.F.** Characteristics and Luminescence of Ge Doped ZnO Films Prepared by Alternate Radio Frequency Magnetron Sputtering *Applied Surface Science* 245 (1–4) 2005: pp. 414–419.  
<http://dx.doi.org/10.1016/j.apsusc.2004.10.037>
  25. **Djurišić, A.B., Leung, Y.H., Choy, W.C.H., Cheah, K.W., Chan, W.K.** Visible Photoluminescence in ZnO Tetrapod and Multipod Structures *Applied Physics Letter* 84 (14) 2004: pp. 2635–2637.  
<http://dx.doi.org/10.1063/1.1695633>
  26. **Yao, B.D., Chan, Y.F., Wang, N.** Formation of ZnO Nanostructures by a Simple Way of Thermal Evaporation *Applied Physics Letters* 81 (4) 2002: pp. 757–759.  
<http://dx.doi.org/10.1063/1.1495878>